



Cathelicidin-BF ameliorates lipopolysaccharide-induced intestinal epithelial barrier disruption in rat



Feifei Han^a, Zeqing Lu^b, Yifan Liu^b, Xi Xia^b, Haiwen Zhang^b, Xinxia Wang^b, Yizhen Wang^{b,*}

^a Food Safety Key Laboratory of Zhejiang Province, School of Food Science and Biotechnology, Zhejiang Gongshang University, Hangzhou, 310018, China

^b Key Laboratory of Animal Nutrition and Feed Science (Hua Dong), Ministry of Agriculture, College of Animal Sciences, Zhejiang University, Hangzhou 310058, China

ARTICLE INFO

Article history:

Received 29 October 2015

Received in revised form 21 March 2016

Accepted 21 March 2016

Available online 24 March 2016

Keywords:

Cathelicidin-BF

Lipopolysaccharide

Tight junction

Intestinal epithelial barrier disruption

ABSTRACT

Aims: The present study examined the effect of the antimicrobial peptide cathelicidin-BF (CBF) on LPS-induced mucosal injury and intestinal epithelial barrier dysfunction in a rat model and in the porcine intestinal epithelial cell line.

Main methods: Changes in barrier integrity were assessed in intestinal epithelium and IPEC-J2 monolayers by measuring nutrient absorption and transepithelial electrical resistance (TER), and the permeability of intestinal epithelium was examined by measuring plasma D-lactate and diamine oxidase levels. The expression levels of tight junction (TJ) proteins were quantified by real-time PCR, and immunofluorescence was used to analyse the location and distribution of TJs in cells.

Key findings: *In vivo*, CBF improved epithelial barrier function through attenuating the alterations of the mucosal structure, nutrient absorption and TER in the jejunum, and preventing the down-regulation of TJ proteins in LPS-induced rat intestinal epithelium. *In vitro*, CBF prevented the disruption and the re-distribution of ZO-1 and occludin, and suppressed the increase in inflammatory cytokine levels in LPS-induced IPEC-J2. The CBF-induced upregulation of zonula occludens-1 and occludin was prevented by U0126 or SB203580, suggesting the involvement of the MEK and p38 MAPK pathways in the CBF-induced changes in tight junctions.

Significance: Our results showed that CBF prevents LPS-induced intestinal epithelial barrier dysfunction, suggesting its potential as a therapeutic agent for the prevention of LPS-mediated intestinal diseases. We found that exogenous CBF had protective effects on LPS-induced intestinal epithelial barrier disruption in rats and on epithelial damage in IPEC-J2 cells.

© 2016 Elsevier Inc. All rights reserved.

1. Introduction

The mucosal epithelium of the intestine forms a continuous monolayer *in vivo*, playing a critical role in the resistance against microbially-triggered gastrointestinal disease. Defects in barrier integrity, which are a pathophysiological feature of mucosal inflammatory diseases, result in increased permeability. Increased permeability, in turn, causes the leakage of water and plasma proteins into the lumen and the translocation of intestinal bacteria and/or microbial byproducts into the systemic circulation, which contributes to the development of systemic septicaemia [16]. Therefore, the maintenance of epithelial barrier integrity is essential for intestinal homeostasis [16,40,41]. The

bacterial endotoxin lipopolysaccharide (LPS), which is produced by Gram-negative bacteria, causes mucosal hyperpermeability *in vivo* [9]. This hyperpermeability is thought to result from the indirect action of LPS on the intestinal epithelium mediated by mechanisms such as mucosal ischaemia. Administration of LPS to IEC-6 cells disrupts the barrier function of tight junctions (TJs), as indicated by transepithelial electrical resistance (TER) [24]. LPS increases the permeability of intestinal epithelial cells, and this reaction is correlated with the redistribution of intestinal TJ-associated proteins [24,51]. *In vivo* and *in vitro* studies in animals and humans suggest that LPS disrupts intestinal barrier function leading to bacterial translocation [10,39,58]. Although many studies have demonstrated the negative effect of LPS on the integrity of the intestinal mucosa, few effective clinical and non-antibiotic therapeutic approaches to counteract LPS-induced intestinal epithelial barrier dysfunction have been identified.

The cathelicidin family consists of antimicrobial peptides characterised by conserved pro-peptide sequences, and the family was first identified in mammals [12]. In mice, mCRAMP peptide of the cathelicidin family expressed in inflammatory and epithelial cells [14]. Mice lacking mCRAMP displayed significantly increased colonisation of *Citrobacter rodentium* on the colonic surface epithelium [18].

Abbreviations: C-BF, cathelicidin-BF; DAO, diamine oxidase; DSS, dextran sulphate sodium; EHEC, enterohemorrhagic *E. coli*; EPEC, enteropathogenic *Escherichia coli*; IPEC-J2, intestinal porcine epithelial cell line J2; JAM, junction adhesion molecule; LPS, lipopolysaccharide; RT-PCR, reverse-transcription polymerase chain reaction; SD, Sprague-Dawley; TER, transepithelial electrical resistance; TJ, tight junction; TJs, tight junction proteins.

* Corresponding author at: College of Animal Sciences, Zhejiang University, 866 Yuhangtang Road, Hangzhou 310058, China.

E-mail address: yzwang@zju.edu.cn (Y. Wang).

Additionally, mCRAMP possesses bactericidal activity against enteropathogenic *Escherichia coli* and enterohemorrhagic *E. coli* [18]. Endogenous cathelicidin modulates dextran sulphate sodium (DSS)-mediated intestinal inflammation in mCRAMP-deficient (*Camp*^{-/-}) mice [26], and mCRAMP administration ameliorates colitis in wild-type mice exposed to DSS [55]. Although antimicrobial peptides such as cathelicidins have the ability to kill microbial pathogens, there is emerging evidence that these peptides possess multiple receptor-mediated functions and are involved in diverse physiological processes, such as cell proliferation and migration, immune modulation, wound healing, angiogenesis, and the release of cytokines and histamines [5,38,46]. Cathelicidins ameliorate *Clostridium difficile* colitis and toxin A enteritis partly by suppressing enterotoxin-induced alterations in mucosal structure in mice [17]. Cathelicidin-BF (CBF), a 30-aa peptide purified from the snake venom of *Bungarus fasciatus*, has high antimicrobial activity and very rapid microbe-killing efficacy [59]. CBF has high antimicrobial activity against Gram-positive and Gram-negative bacteria and low cytotoxicity [29]. In previous work from our group, we showed that CBF attenuates dextran sulphate sodium-induced ulcerative colitis by regulating intestinal immunity and intestinal barrier function. Inhibition of NF- κ B (p65) phosphorylation was involved the correlative process [61]. After then, the results from Song et al. also showed C-BF pretreatment significantly weakened LPS induced increases in permeability to large molecules mucosal, morphological damage and epithelial ZO-1 disruption in a mouse model of endotoxemia. C-BF also reduced LPS induced TNF- α expression through the NF- κ B signalling pathway in mouse RAW264.7 macrophages [50]. However, the effect of CBF on the maintenance and re-establishment of intestinal barrier function in rat jejunum and intestinal epithelial cell monolayers remains unclear. Transepithelial electrical resistance (TER) is a widely accepted quantitative technique to measure the integrity of tight junction dynamics and their values are strong indicators of the integrity of the cellular barriers. Nutrient absorption and TER were measured in this study to assess epithelial barrier function in rats and IPEC-J2 cells. Furthermore, we examined the effects of CBF on LPS-induced alterations of intestinal mucosal architecture, epithelial barrier disruption, reduction of ZO-1 and occludin distribution in a rat model and porcine IPEC-J2 cells. Otherwise, proinflammatory cytokines such as TNF- α , IL-8, and IFN- γ are released within the intestinal mucosa during the development of LPS-induced enteropathies. These proinflammatory cytokines have been shown to disrupt intestinal epithelial barrier function both *in vitro* and *in vivo* [2,28]. We also investigated whether the proinflammatory cytokines involved the process of CBF modulating tight junctions in rat.

2. Materials and methods

2.1. Preparation of CBF

CBF was synthesised and purified by Chinese peptides company (Hangzhou, China), and the molecular weight of the purified CBF was confirmed by matrix-assisted laser desorption/ionisation time-of-flight mass spectroscopy (Model Autoflex, Bruker Daltonics Inc., USA) using α -cyano-4-hydroxycinnamic acid as the matrix. The purity of the peptide was determined to be >95% by analytical reverse phase-HPLC. The peptide was then dissolved in pure water at a concentration of 3.0 mg/mL, and the peptide solution was stored at -80°C until use.

2.2. Animals and design of *in vivo* experiments

Male Sprague-Dawley (SD) rats (10–12 weeks) were obtained from Zhejiang Provincial Center for Disease Control and Prevention (Zhejiang CDC, Hangzhou, China). Animals were individually housed and maintained on a 12:12 h light-dark cycle under specific pathogen-free conditions. Ten rats per group were used in all animal experiments and animals were provided with food and water *ad libitum*. Animal experimental procedures were approved by the Committee on the Ethics of

Animal Experiments of Zhejiang University (Permit Number: SYXK 2012-0178).

To assess whether CBF has a protective effect on intestinal epithelial barrier function, 10-week-old male SD rats (10 per group) were randomly selected. Three groups of rats received 0, 5, or 10 mg/kg (mg per kg body weight) of CBF in a total volume of 800 μL sterile saline by intraperitoneal injection. After 20 h, rats were injected with 200 μL sterile saline containing 5 mg/kg of *E. coli* LPS (Sigma-Aldrich, St. Louis, MO) and were observed for 4 h after the treatment with LPS (LPS and CBF + LPS groups). To assess whether CBF has a healing effect on intestinal epithelial barrier disruption, two groups of rats were intraperitoneally injected with 5 mg/kg of *E. coli* LPS in 200 μL sterile saline for 4 h, followed by injection of 5 or 10 mg/kg of CBF for 20 h (LPS + CBF groups). Ten rats that received 800 μL sterile saline for 24 h and then 200 μL of sterile saline for 4 h were used as the control group. Two groups of rats receiving 5 or 10 mg/kg of CBF for 24 h were used as CBF controls. The rats were anaesthetised by intraperitoneal injection of 15 mg/kg of sodium pentobarbital and blood was collected. The rats were then euthanized by cervical dislocation and the jejunum was rapidly removed and used for further experiments.

2.3. Assessment of histopathological changes and immunohistology

For histological measurements, tissues from at least four rats in each group (2–4 sections per rat) were examined. Full thickness sections of the middle jejunum were excised, immediately fixed in neutral-buffered formalin, stained with haematoxylin-eosin (H&E), and embedded in paraffin. H&E-stained sections of 5 μm were used for measurements. The villus height and crypt depth were measured directly under a Leica NEWDM 4500BR microscope using an ocular lens with a micrometer. At least 10 measurements from non-overlapping, well-oriented areas were obtained from each sample, and the results were expressed in micrometers.

Segments of the jejunum were frozen in liquid nitrogen immediately after removal and stored at -80°C until used. Frozen sections were mounted on the poly-L-lysine-coated slides. Then the slides were dried and fixed in 4% buffered paraformaldehyde (pH 7.4) for 10 min at room temperature. Fixed sections were washed in PBS and blocked with 1% bovine serum albumin (BSA) in PBS for 20 min at room temperature. The slides were incubated with anti-ZO-1 or occludin antibodies (both from Abcam, Cambridge, UK) overnight at 4°C . Negative controls were processed similarly using BSA in PBS instead of primary antibody. After washing, the sections were incubated with goat anti rabbit antibody conjugated with FITC (Jackson ImmunoResearch Laboratories, USA). Nuclei were counterstained with DAPI (Sigma-Aldrich, MA, USA). Finally, the sections were viewed with a fluorescence microscope (Nikon 108, Japan).

2.4. Plasma D-lactate and DAO levels

After treatment, rats were anaesthetised by intraperitoneal injection of 15 mg/kg of sodium pentobarbital and 3 mL of venous blood was collected. The plasma was deproteinised with perchloric acid, and the levels of D-lactate and diamine oxidase (DAO) in the plasma were detected by spectrophotometry using Multi-Mode Microplate Readers, as described by Sun [53] and Jin [19] (SpectraMax M5, Molecular Devices, USA).

2.5. Cell culture and treatment

The small intestinal porcine epithelial cell line J2 (IPEC-J2) (donated by Dr. Junjun Wang, China Agricultural University, Beijing, China), which was isolated from the epithelium of the jejunum of a neonatal unsuckled piglet, was characterised and used as an *in vitro* model system in this study [44]. IPEC-J2 cells were maintained in culture as described previously [45]. IPEC-J2 cells were grown in dishes at a density

Table 1
Primers used in the quantitative real-time PCR.

Target gene	GenBank accession no.	Primer sequence (5'-3')	Product size (bp)
Claudin-1	NM031699.2	ATTGGCATGAAGTGCATGAG CCATGGCCTCCCTGGCGTC	108
Occludin	NM031329.2	ACACAGACCCCAGAGCGGCA AGCCTGGGAGTCCGGTTGA	218
ZO-1	NM001106266.1	GCCAGCCAGTTCGGCTCTG AGGGTCTCCCGGGTTGGTG	173
JAM-1	NM053796.1	GCGAAGCTGTCCACGCGGA CGCAGTGGTGTGCTCTGGA	265
IFN- γ	NM_213948.1	CAAAGCCATCAGTGAACCTCATCA TCTCTGGCCTGGAACATAGTCT	100
IL-8	NM_003361958	TTCCGATGCCAGTGATAAATA CTGTACAACCTTCTGCACCCA	176
NF- κ B (p65)	NM_001048232	CTCGACAAGGAGACATGAA ACTCAGCCGGAAGGCATTAT	147
TLR4	NM_001113039.1	GCCATCGCTGTAACATCATC CTCATACTCAAAGATACACCATCCG	108
TNF- α	NM_214022.1	CCAATGGCAGAGTGGGTATG TGAAGAGGACCTGGGAGTAG	116
18S	NR046237.1	GTAACCCGTTGAACCCATT CCATCCAATCGGTAGTAGCG	151

of 1×10^6 cells per well and randomly divided into groups to measure the distribution of TJ proteins and mRNA expression as follows: control group (treated with sterile saline), LPS group (treated with 1 μ g/mL LPS for 4 h), and CBF + LPS group (treated with 10 μ g/mL CBF for 20 h before exposure to 1 μ g/mL LPS for 4 h). For the analysis of cytokine mRNA and protein levels, IPEC-J2 cells were divided into the following four groups: control (untreated), LPS (treated with 1 μ g/mL LPS for 4 h), CBF (treated with 10 μ g/mL CBF for 24 h), and CBF + LPS (treated with 10 μ g/mL CBF for 20 h before exposure to 1 μ g/mL LPS for 4 h). To detect signalling pathways, parental epithelial cells were preincubated for 1 h with 10 μ M of the MEK inhibitor U0126, or 10 μ M of the p38 MAPK inhibitor SB203580, before treatment with 10 μ g/mL CBF for 24 h either alone or in combination. Cells were harvested at the indicated time points.

2.6. Transmission electron microscopy (TEM)

Approximately 5×10^5 cells were seeded onto 1.13 cm² permeable supports (Snapwell, Costar, Corning Incorporated). Monolayers of cells were fixed with 2.5–3.0% glutaraldehyde (Polyscience, USA) in 0.1 M cacodylate buffer (pH 7.2–7.4, Agar scientific, UK) for 1 h at room temperature and rinsed twice with cacodylate buffer adjusted to 300 mOsm with 6.84% sucrose. The cells were then subjected to post-fixation with 1% osmium tetroxide in cacodylate buffer for 1 h at 4 °C and rinsed twice with cacodylate-sucrose buffer. Monolayers were dehydrated in a graded ethanol series and embedded with white resin. Specimens were stained with uranyl acetate and alkaline lead citrate for 15 min and observed by TEM (Model JEM-1230, JEOL, Japan).

2.7. Electrophysiology measurements

Short-circuit current (I_{sc}) and transepithelial electrical potential were measured using a modified Ussing chamber (VCC MC6, PI) as described previously [1,42]. Jejunum tissue from rats and *in vitro* monolayers were immediately immersed in oxygenated Krebs buffer (pH 7.4) and mounted into Ussing chambers (World Precision Instruments; Narco Scientific, Mississauga, Ontario, Canada). The chamber exposed 0.6 cm² of tissue surface area to 8 mL of circulating oxygenated Krebs buffer at 37 °C. The serosal buffer (pH 7.4) also contained 10 mM glucose as an energy source that was osmotically balanced by 10 mM mannitol in the mucosal buffer (pH 7.4). The chambers contained agar-salt bridges to monitor the potential difference across the tissue and to inject the required I_{sc} to maintain a zero potential difference, as registered with an automated voltage clamp. Tissue

conductance, representing passive permeability to ions, was calculated by Ohm's law. The baseline values for I_{sc}, indicating net ion secretion, and the conductance, as an inverse measure of tissue resistance, were recorded at equilibrium, which was 20 min after the mounting of the intestinal segments.

2.8. RNA isolation and qRT-PCR

Total RNA isolation and cDNA synthesis by reverse transcription were performed using the TRIzol reagent (Invitrogen Corporation, Carlsbad, CA) and the M-MuLV reverse transcriptase kit (Fermentas, EU, Glen Burnie, Maryland, USA), respectively. The mRNA levels of individual genes were measured by real-time PCR using a SYBR® Premix Ex Taq™ Kit (Takara Biotechnology Co., Ltd., Otsu, Shiga, Japan) in the ABI StepOne Plus™ Real-Time PCR system (Applied Biosystems, Foster City, CA, USA). Real-time PCR reactions were performed as follows: a pre-cycling stage at 95 °C for 30 s, then 40 cycles of denaturation at 95 °C for 10 s and annealing at 60 °C for 34 s. Fluorescence was measured at the end of each annealing step, and the melting curves were monitored to confirm the specificity of the PCR products. Data were analysed according to the comparative threshold cycle (C_t) method and normalized to an endogenous reference (18S ribosome protein gene). The primers used in this experiment are listed in Table 1.

2.9. Western blotting and immunofluorescence staining

Polarised IPEC-J2 cells grown on Transwell supports were lysed by gently scraping the cells into buffer containing a complete protease inhibitor cocktail. The protein content of each monolayer was quantified using the bicinchoninic acid (BCA) protein assay reagent kit (Pierce Chemicals, Rockford, USA) and diluted to ensure that 15 μ g of protein was loaded in each lane of a 7.5%/10% SDS-PAGE gel. Proteins were separated by SDS-PAGE, transferred to nitrocellulose membranes, blocked with 5% (w/v) dry milk in TBS and incubated with primary antibodies overnight at 4 °C. An HRP-conjugated secondary antibody was then applied before the proteins were visualised by the chemiluminescence method.

The concentrations of TLR-4 and NF- κ B (p65) in extracts from IPEC-J2 monolayers were determined using the Coomassie brilliant blue assay. Extracts containing equal amounts of proteins (100 μ g) were electrophoresed in SDS-PAGE gels, transferred to PVDF membranes, which were blocked for 30 min in 5% skimmed milk in PBS and then incubated overnight at 4 °C with antibodies against c-Jun, TLR-4, NF- κ B p65, NF- κ B p-p65 (Santa Cruz Biotechnology Inc., Santa Cruz, California,

USA). Blots were developed with enhanced chemiluminescence detection reagents (Santa Cruz), exposed on Kodak Xmat blue XB-1 film, and quantified by Bandscan 5.0 software using GAPDH as the internal control.

The IPEC-J2 monolayers were rinsed with pre-warmed HBSS for 5 min and subsequently permeabilised, stained, and fixed. For ZO-1 and occludin labelling, monolayers were permeabilised with cold methanol (-20°C) for 30 min. Non-specific binding sites were blocked with PBS containing 1% w/v BSA for 10 min. The cells were then immunoprobed with 2.5 $\mu\text{g}/\text{mL}$ of a rabbit anti ZO-1 antibody, a rabbit anti-occludin antibody (Abcam, Cambridge, UK) or PBS (negative control) for 1 h. Each well was washed three times with 1% BSA-PBS for 5 min prior to being incubated with 5 $\mu\text{g}/\text{mL}$ of a FITC-conjugated goat anti-rabbit antibody for 1 h protected from light. The monolayers were washed five times with 1% BSA-PBS for 5 min and post-fixed with 4% w/v paraformaldehyde in PBS for 10 min. The filters were removed from the plastic supports, mounted on slides with Vectashield containing DAPI, and examined on a Leica TCS SP5 confocal laser microscope.

2.10. Statistical analysis

All experiments were performed at least three times unless otherwise indicated. SPSS 18.0 (IBM Inc., Chicago, IL, USA) was used for the

statistical analysis. The results are expressed as the means \pm standard error of the mean (SEM) of all samples. Statistical differences among groups were analysed using one-way analysis of variance (ANOVA) followed by Fisher's least significant difference (LSD) and Duncan as a multiple comparison test. A value of $P < 0.05$ was considered to be statistically significant.

3. Results

3.1. CBF attenuates LPS-induced alterations of the jejunal mucosal architecture

To assess the potential role of CBF in LPS-induced intestinal mucosal architecture, SD rats (10 rats in each group) were treated by intraperitoneal injection of LPS before or after CBF administration. As shown in Fig. 1, rats treated with LPS developed intestinal epithelial disruption with altered mucosal architecture. However, CBF treatment after or before LPS significantly decreased LPS-induced damage to the jejunal mucosa, as shown by H&E staining (Fig. 1A). Villus height decreased significantly and crypt depth increased significantly in the LPS-treated group (Table 2). Administration of 10 mg/kg CBF after or before LPS injection significantly improved villus height and decreased crypt depth (Table 2). TEM revealed that CBF administration attenuated the obvious pathological changes in the intestinal mucosa caused by LPS (Fig. 1B),

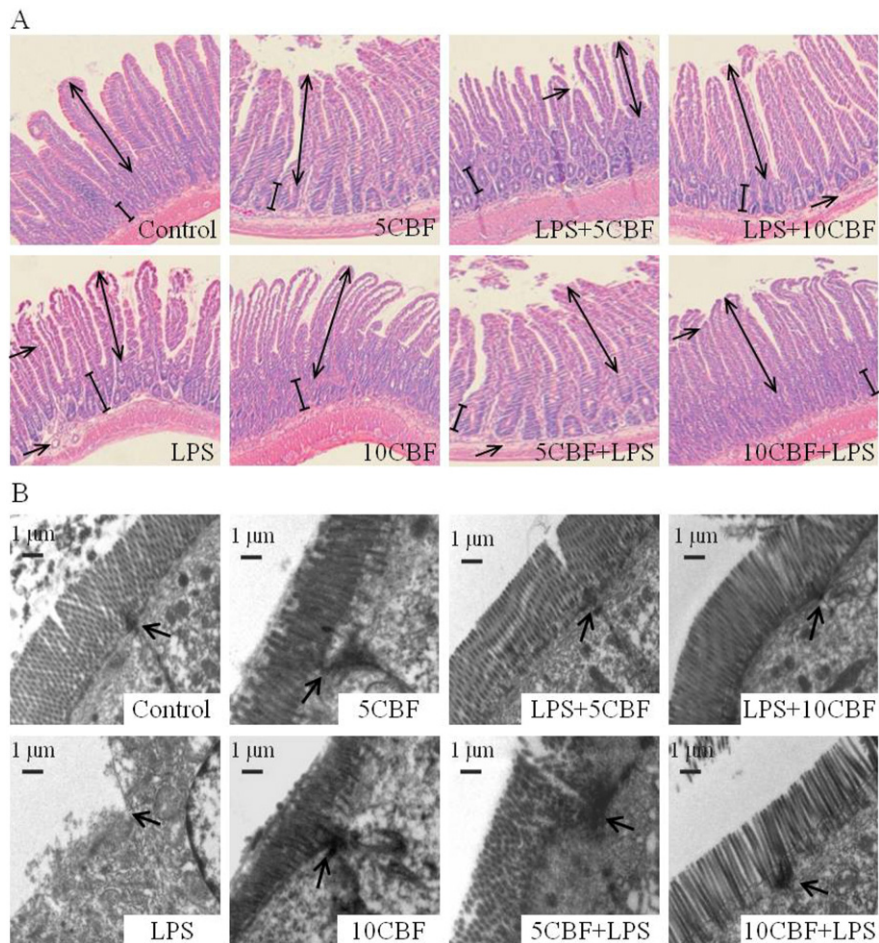


Fig. 1. Alterations in the architecture of the jejunal mucosa of rats treated with LPS alone or LPS together with CBF (5 or 10 mg/kg CBF). A: H&E staining of the mucosa of the jejunum ($\times 40$). The single sided arrow (\rightarrow) indicates morphological changes of mucous layer. The double sided arrow (\leftrightarrow) indicates villus height. The line segment ($|$ — $|$) indicates crypt depth. Take LPS + 10CBF group as example, 10CBF significantly improved LPS-induced villus shorten, disordered arrangement of intestinal epithelial cells and edema status in submucosa. (B) Transmission electron microscopy of epithelial cell microvilli and tight junctions (TJs) (\rightarrow) ($\times 10,000$). The images show the reverse effect of various concentrations of CBF or the administration sequence of LPS and CBF on LPS-induced alteration of microvilli and TJs. Control: control rats with no LPS and CBF treatment. LPS: rats treated with LPS alone. LPS + 5CBF, LPS + 10CBF: rats administrated 5 or 10 mg/kg CBF after the treatment with LPS respectively. 5CBF + LPS, 10CBF + LPS: rats with administration of LPS after 5 or 10 mg/kg CBF administration.

Table 2
Morphometry for jejunum mucosa epithelial morphology in rats¹.

Group	Villus height	Crypt depth	Ratio of villus height and crypt depth
Control	290.23 ± 3.53 ^a	120.29 ± 3.11 ^e	2.41 ± 0.06 ^a
LPS	155.03 ± 3.13 ^e	217.29 ± 1.69 ^a	0.71 ± 0.02 ^e
5 mg/kg CBF	235.57 ± 1.69 ^b	118.64 ± 2.75 ^e	1.76 ± 0.03 ^c
10 mg/kg CBF	237.98 ± 1.32 ^b	134.35 ± 1.07 ^d	2.15 ± 0.06 ^b
LPS + 5 mg/kg CBF	139.29 ± 3.68 ^f	130.84 ± 3.60 ^d	1.16 ± 0.05 ^d
LPS + 10 mg/kg CBF	194.61 ± 5.75 ^d	181.78 ± 5.15 ^b	1.70 ± 0.04 ^c
5 mg/kg CBF + LPS	214.12 ± 2.33 ^c	161.90 ± 1.53 ^c	1.32 ± 0.02 ^d
10 mg/kg CBF + LPS	298.23 ± 2.20 ^a	166.66 ± 3.55 ^c	2.17 ± 0.09 ^b

¹ Mean ± SEM. Values in the same column with different superscripts are significantly different ($P < 0.05$, $n = 10$).

including disarranged and distorted epithelial cell microvilli and disrupted TJ architecture (as indicated by the arrow) due to swollen or shrunken epithelial cells. Groups treated with CBF showed slightly shrunken epithelial cells and a greater number of intact TJs than the LPS-treated group (Fig. 1B).

3.2. CBF promoted the recovery of epithelial barrier function in rats

To determine whether CBF affects epithelial barrier function, we examined the effect of CBF on epithelial permeability, absorption ability, and the TER of the small intestine in rats with LPS-induced intestinal epithelial barrier disruption by evaluating changes in plasma D(–)-lactate

level and DAO. The plasma D(–)-lactate level is a useful marker for assessing intestinal injury and monitoring increases in intestinal permeability following severe injuries [53]. DAO is also often used to evaluate intestinal injury [27] and intestinal permeability [19]. As shown in Fig. 2A, significantly lower concentrations of plasma D(–)-lactate were detected in rats treated with 10 mg/kg of CBF after LPS (0.26 mM) or before LPS (0.28 mM) injections compared with the LPS-treated group (0.42 mM). A similar plasma D(–)-lactate concentration was detected in the control group (0.28 mM). Consistent with these results, 10 mg/kg CBF treatment after LPS (2.7×10^{-3} U/mL) or before LPS (1.7×10^{-3} U/mL) injection resulted in significantly lower levels of DAO than those in the LPS-treated group (3.4×10^{-3} U/mL), and these values were closer to those of the control group (1.7×10^{-3} U/mL) (Fig. 2B). The effects of CBF on LPS-induced hyper-permeability were further tested in a nutrient absorption and TER assay. LPS treatment significantly decreased nutrient (glucose, phosphorus, and glutamine) absorption (Fig. 2C) and TER in the jejunum (Fig. 2D). Treatment with CBF after or before LPS challenge significantly reversed the LPS-induced reduction of nutrient absorption and TER in the jejunum.

3.3. Effect of CBF on the expression of tight junction proteins in LPS-treated rats

LPS disrupts epithelial barrier integrity by downregulating TJ proteins [48]. Therefore, we examined the effect of CBF on the expression of TJ proteins. In LPS-treated rats, the expression levels of claudin-1, occludin, ZO-1, and junction adhesion molecule (JAM) in the jejunum

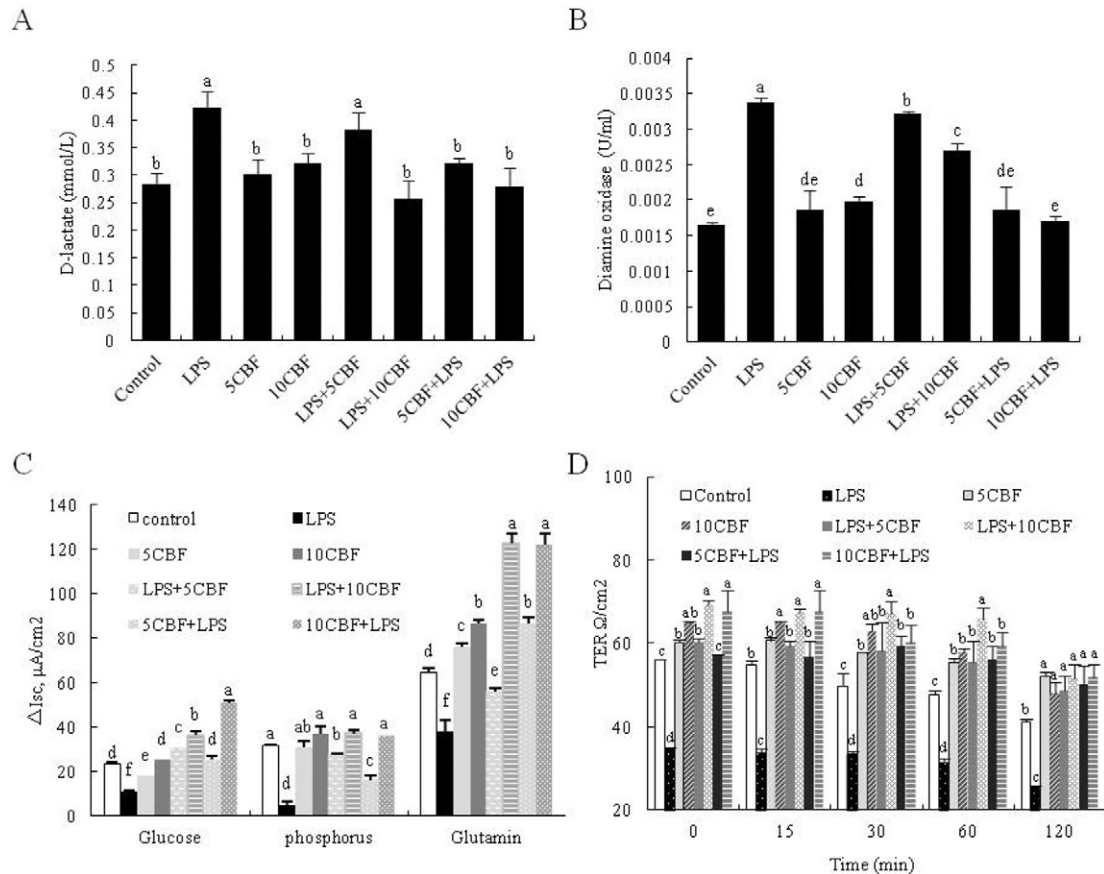


Fig. 2. CBF reverses the effects of LPS on epithelial barrier function in rats. (A) CBF (10 mg/kg) administered either before or after LPS caused the strongest reduction in plasma D-lactate level. (B) CBF (10 mg/kg) significantly reduced the LPS-induced increase of DAO. (C) CBF reversed the LPS-induced reduction of nutrient absorption in jejunum. (D) CBF ameliorated the LPS-induced reduction of TER in jejunum. Control: control rats with no LPS and CBF treatment. LPS: rats treated with LPS alone. LPS + 5CBF or LPS + 10CBF: rats administrated 5 or 10 mg/kg CBF after the treatment with LPS respectively. 5CBF + LPS or 10CBF + LPS: rats with administration of LPS after 5 or 10 mg/kg CBF administration. Data were expressed as the mean ± SEM of six independent assays. Within the different treatments or at the same time point, different letters mean significant differences at $P < 0.05$.

were significantly reduced compared with the control group (Fig. 3A and B). However, compared with LPS groups, co-treatment with CBF prevented the LPS-induced downregulation of these tight junction proteins. Compared with LPS + CBF groups, CBF + LPS groups showed higher expression levels of claudin-1, occludin, ZO-1, and JAM, and treatment with 10 mg/kg CBF was most effective. Because this effect

could be mediated by reinforcement of tight junctions, we investigated whether treatment with CBF interferes with changes in the tight junction protein ZO-1 or occludin production and distribution. Immunohistochemical analysis showed that CBF treatment before LPS completely prevented the loss of expression and changes in distribution of occludin (Fig. 3C) and ZO-1 (Fig. 3D) in the rat jejunum.

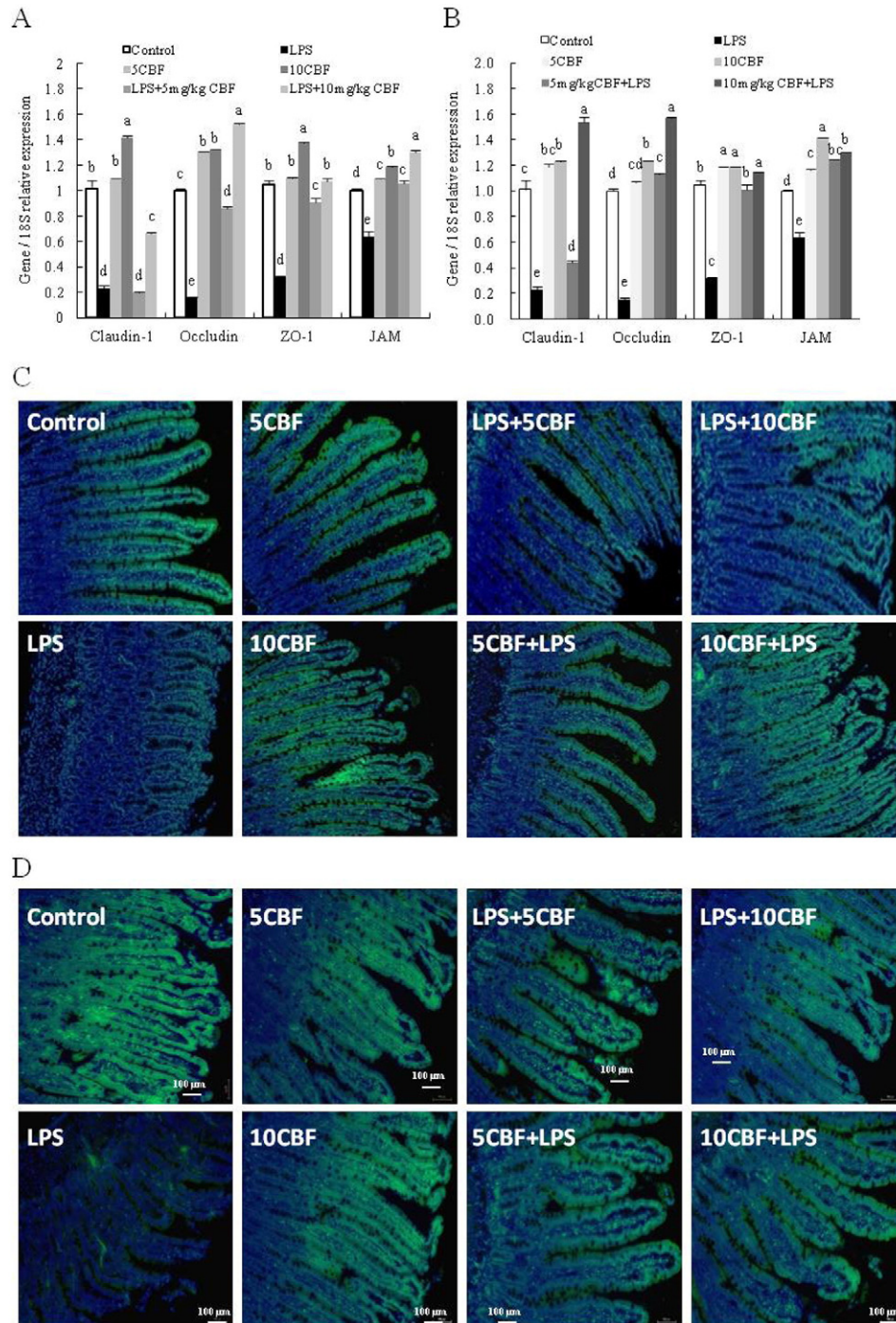


Fig. 3. CBF prevents the LPS-induced downregulation of tight junction proteins. (A) Expression of tight junction (TJ) proteins in the mucosa of the jejunum of rats treated with LPS, LPS + 5 CBF or LPS + 10 CBF. CBF (5 mg/kg) significantly improved the LPS-induced downregulation of occludin, ZO-1 and JAM-1. CBF (10 mg/kg) significantly improved the LPS-induced downregulation of four TJ proteins. (B) Expression of TJ proteins in the jejunum mucosa of rats treated with LPS, 5 CBF + LPS and 10 CBF + LPS. Preadministration of CBF (5 mg/kg or 10 mg/kg) significantly improved LPS-induced downregulation of four TJ proteins. The mRNA levels of TJ proteins was analysed by qRT-PCR and is normalized to 18S ribosome protein mRNA. Values represent the mean \pm SEM of six independent assays. Within each gene, values without a common letter differ, $P < 0.05$. Immunohistological detection of the TJ proteins occludin (C) and ZO-1 (D) in representative sections of jejunum from Control (control rats with no LPS or CBF treatment), LPS (rats treated with LPS alone), LPS + 5CBF or LPS + 10CBF (rats administrated 5 or 10 mg/kg CBF after the treatment with LPS respectively), 5CBF + LPS or 10CBF + LPS (rats with administration of LPS after 5 or 10 mg/kg CBF administration). Fluorescent signal of occludin or ZO-1 (green) is merged with DAPI counterstained nuclei (blue).

3.4. CBF diminishes the LPS-induced disruption in barrier function in IPEC-J2 cells

To confirm the *in vivo* findings, we further assessed the effect of CBF on barrier function in porcine IPEC-J2 cells. TJs were disrupted in IPEC-J2 cells treated with LPS, whereas there was no obvious disruption of TJs in the CBF + LPS group compared with the control group (Fig. 4A). Consistent with our *in vivo* study, the absorption of nutrients (glucose, phosphorus, copper, and glutamine) significantly decreased following LPS treatment, whereas CBF treatment restored nutrient absorption to the levels observed in the control group (Fig. 4B). In addition, LPS exposure resulted in a rapid decrease in TER in the IPEC-J2 cell monolayer, whereas TER was restored in cells treated with CBF + LPS (Fig. 4C), which showed a slower decrease similar to that of the control group.

3.5. CBF prevents LPS-induced re-distribution and reduction of TJs in IPEC-J2 cell monolayers

To explore the possible mechanisms underlying the protective effect of CBF in IPEC-J2 cell monolayers after LPS treatment, the expression of the TJ associated proteins ZO-1 and occludin was assessed. LPS significantly downregulated ZO-1 and occludin at the mRNA (Fig. 5A) and protein levels (Fig. 5B) compared with those in the control group, whereas CBF significantly inhibited the LPS-induced downregulation of occludin and ZO-1. Immunofluorescence and confocal imaging analyses were used to determine the localisation of tight junction-associated ZO-1 and occludin in LPS-treated IPEC-J2 cells, which showed that LPS induced a decrease in the levels of occludin (Fig. 5C) and ZO-1 (Fig. 5D) in the junctional areas after 4 h of incubation. By contrast, pre-incubation with CBF resulted in significantly higher expression of occludin and ZO-1, with normal protein distribution compared with that in LPS-treated cells. The junctional proteins appeared to be localised to the cytosolic area and nucleus of the cells (Fig. 5C, 5D).

3.6. CBF counteracts the LPS-induced dysregulation of cytokine levels

To better understand the mechanism underlying the effect of CBF, we investigated the potential involvement of cytokine dysregulation in the LPS-induced reduction and re-distribution of TJs. Specifically, we analysed the gene expression and secretion levels of TNF- α , IL-8, and IFN- γ (Fig. 6A and B). LPS upregulated TNF- α , IL-8, and IFN- γ , whereas treatment with 10 μ g/mL CBF for 20 h before exposure to LPS restored the expression of TNF- α , IL-8, and IFN- γ mRNA and protein to normal levels. Single treatment with 10 μ g/mL CBF did not have a significant impact on TNF- α , IL-8, and IFN- γ expression levels. LPS-induced secretion of TNF- α and IL-8 may occur via a distinct TLR-4/NF- κ B pathway; therefore, we quantified the expressions levels of TLR-4 and NF- κ B. (Fig. 6A and C). LPS stimulation upregulated TLR-4 and NF- κ B gene expression and TLR-4 and phosphorylated NF- κ B p65 protein expression. However, CBF (10 μ g/mL) potently inhibited the increases in mRNA and protein levels of TLR-4 and phosphorylated NF- κ B p65 induced by LPS, as well as the signalling pathways downstream of the cytokines in LPS-stimulated epithelial cells.

3.7. Mitogen-activated protein kinase (MAPK)/extracellular regulated kinase (ERK) kinase (MEK), and p38 MAPK inhibitors block changes in the expression of adherens and tight junctions caused by CBF

To determine whether the MEK and p38 MAPK pathways are involved in the CBF induced changes in tight junctions, cells were treated with the specific inhibitors U0126 or SB203580 for 1 h. The effects of treatment with U0126 or SB203580 on the CBF-induced upregulation of tight junction proteins were examined by qRT-PCR and western blotting. Treatment with CBF upregulated occludin and ZO-1 in IPEC-J2 cells after treatment for 24 h (Fig. 7A and B). In IPEC-J2 cells treated with U0126 or SB203580, occludin mRNA and protein levels decreased significantly ($P < 0.05$), whereas expression of ZO-1 returned to half the level of control cells (Fig. 7A and B).

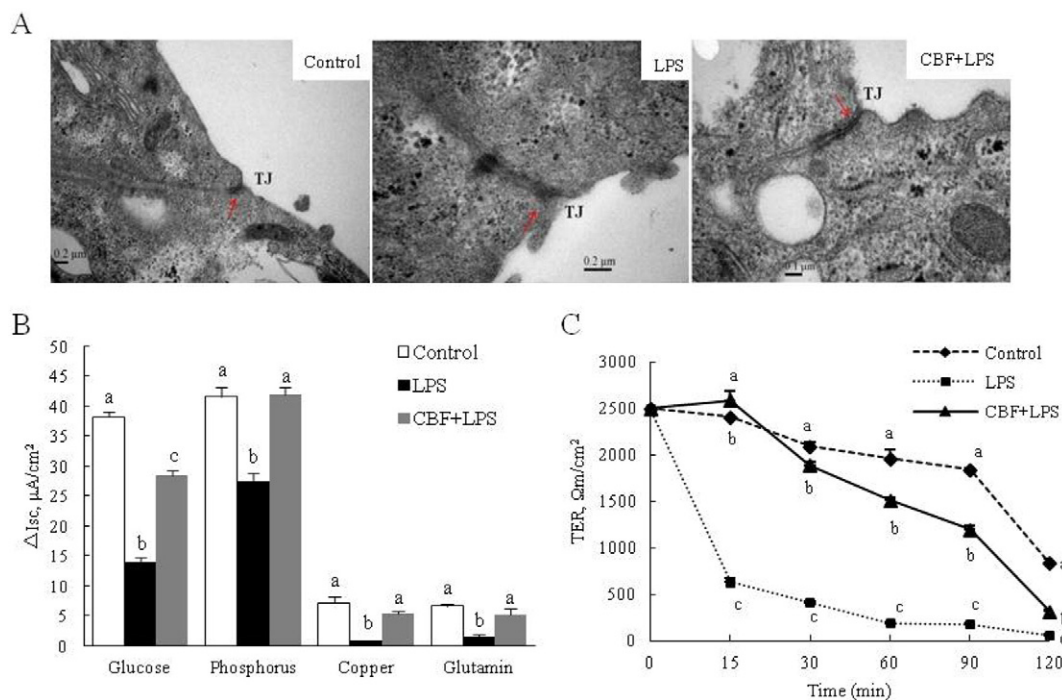


Fig. 4. CBF diminishes LPS-induced disruption of TJs and integrity of IPEC-J2 cell monolayers. (A) Transmission electron microscopy of TJs in IPEC-J2 from the control, LPS and CBF + LPS groups. Control group, TJs (\rightarrow) were intact; LPS group, TJs (\rightarrow) were disrupted; CBF + LPS group, TJs (\rightarrow) were intact. (B) ΔI_{sc} in IPEC-J2 from the control, LPS and CBF + LPS groups. CBF reversed LPS-induced decrease in nutrient absorption. Different letters mean significant differences at $P < 0.05$. (C) TER in IPEC-J2 from the control, LPS and CBF + LPS groups. LPS exposure resulted in a rapid decrease in TER in IPEC-J2 cell monolayer, whereas CBF treatment led to much slower decrease in TER. Control: treated with sterile saline, LPS group: treated with 1 μ g/mL LPS for 4 h, CBF + LPS: IPEC-J2 treated with treated with 10 μ g/mL CBF for 20 h before exposure to 1 μ g/mL LPS for 4 h. Values represent the mean \pm SEM of six independent assays. Within the different treatments or the same time point, different letters mean significant differences at $P < 0.05$.

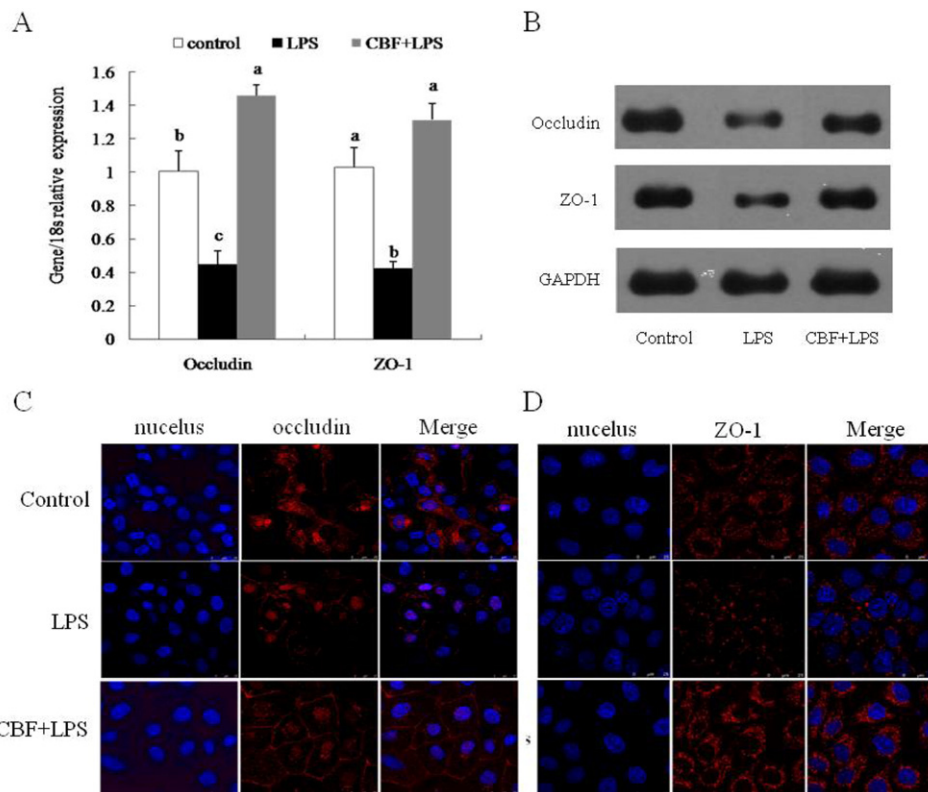


Fig. 5. CBF inhibits LPS-induced downregulation and re-distribution of occludin and ZO-1. Administration of CBF significantly prevented the LPS-induced downregulation of occludin and ZO-1 at the mRNA (A) and protein (B) levels. Different letters mean significant differences at $P < 0.05$. The occludin (C) and ZO-1 (D) proteins were distributed normally compared to those in LPS-treated cells after a pre-incubation with CBF as examined by immunofluorescence microscopy.

4. Discussion

Epithelial disruption has been associated with the pathogenesis of a number of diseases induced by intestinal pathogens and/or bacterial enterotoxins [8,20,23,32,48,57]. Despite extensive evidence of the disruptive effects of LPS on epithelial integrity and TJ structure [7,11,24,48], effective clinical therapeutic approaches remain largely unidentified. In the present study, the effect of the antimicrobial peptide CBF on attenuating the detrimental effects of LPS on epithelial barrier function was demonstrated *in vivo* and *in vitro*. The mucosal structure of the small intestine is markedly altered after treatment with LPS [11], and this effect includes the disruption of tight junctions [51]. In the present study, we confirmed that severe damage to the intestinal mucosa occurs after LPS treatment in the jejunum of rats. CBF could prevent (administered before LPS) LPS-induced intestinal damage, which have the consistent conclusion with the mice model investigated in our lab previous study [50]. However, we proved CBF rescued (administered after LPS) the LPS-induced rat intestinal damage in this study. The disruption of the integrity of the intestinal mucosa in LPS-treated rats was indicated by impaired absorption of nutrients and decreased TER. The degree of intestinal permeability caused by endotoxins is variable, and the mechanism behind this phenomenon may be related to different inflammatory mediators, such as cytokines, vasoactive amines, and free radicals [33,35]. The increased intestinal permeability in animals fed with total parenteral nutrition (TPN) is primarily caused by atrophy of the intestinal mucous membrane [31,52]. Therefore, the impaired nutrient absorption and decreased TER in the LPS group could have been associated with damage to the intestinal mucosa. In animals treated with CBF, the morphologic alterations to the intestinal mucosa (including shedding of epithelial cells, fracturing of villi, mucosal atrophy, and TJ disruptions) were significantly alleviated, which may have attenuated LPS-induced damage to the intestinal mucous membrane, consistent

with the improvement in nutrient absorption and TER. The positive effect of CBF on TER was associated with a significant increase in microvillus length and crypt depth in the jejunum of rats.

Since TER is an indicator of the degree of integrity of TJs, we further investigated the relative mRNA expression of TJ components, including claudin-1, occludin, ZO-1, and JAM, using qRT-PCR. We found that the mRNA levels of claudin-1, occludin, ZO-1, and JAM were significantly reduced in the LPS treatment group compared with the control group, which is consistent with previous reports. Sheth et al. showed that LPS induces the redistribution of tight junction proteins, including occludin, claudin-1, claudin-4, and ZO-1, from the intercellular junctions and reduces the levels of ZO-1 [48]. However, co-treatment with CBF and LPS significantly upregulated these proteins as the mRNA level, especially at a high CBF concentration of 10 mg/kg. This result suggests that modulation of the mRNA expression of TJ components may be one of the mechanisms by which CBF improved epithelial barrier function in LPS-treated rats. This mechanism may also explain the protective (administration before LPS) and healing (after LPS) effects of CBF on epithelial permeability, especially at the concentration of 10 mg/kg. The protective effect of CBF on LPS-induced intestinal barrier disruption was further confirmed in an *in vitro* model using the IPEC-J2 cell line. This cell line conserves its epithelial nature and has been used as an *in vitro* model to study porcine intestinal pathogen-host interactions and porcine-specific pathogenesis [4]. It can also serve as a model to stimulate the innate immune function of the intestinal epithelium [15]. LPS disrupted barrier function and increased paracellular permeability in IPEC-J2 cell monolayers, and CBF attenuated the LPS-induced alteration of TJs and increased nutrient absorption and TER in IPEC-J2 cells. These *in vitro* results were consistent with our *in vivo* results.

To further elucidate the mechanism mediating the protective effect of CBF on barrier function in IPEC-J2 cells, we investigated the role of the TJ-associated proteins occludin and ZO-1. Occludin and ZO-1 are

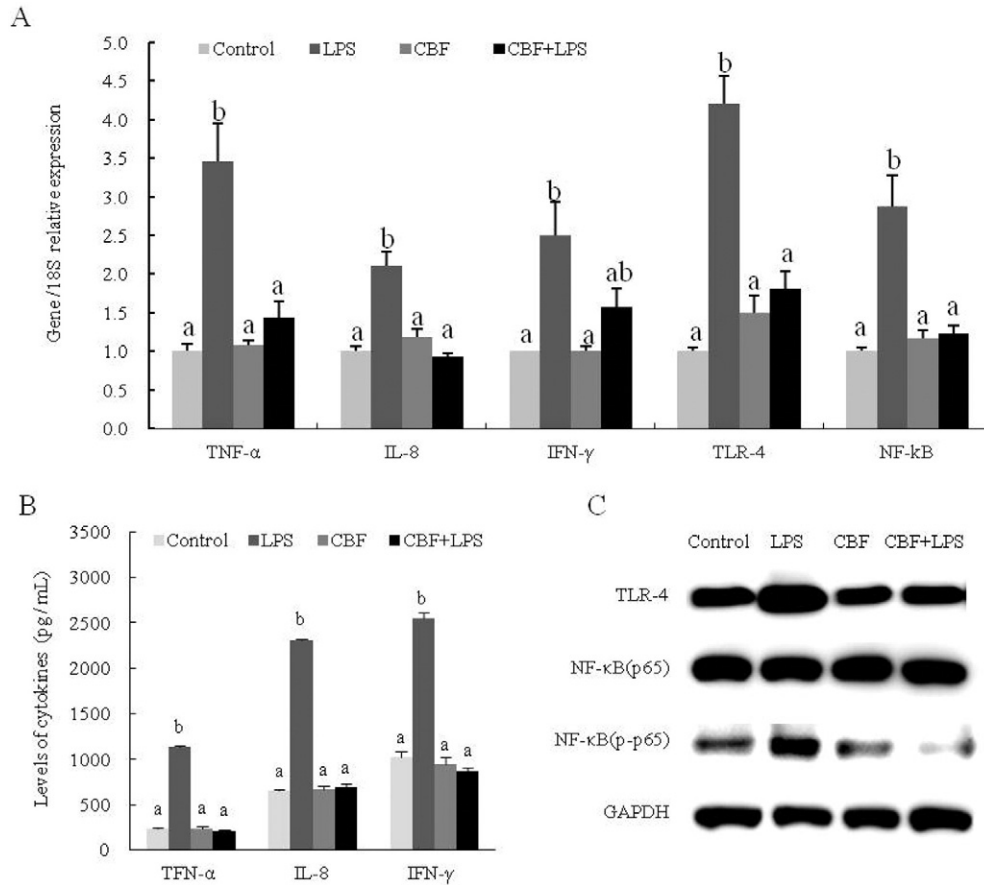


Fig. 6. CBF prevents LPS-induced dysregulation of TNF-α, IL-8, IFN-γ, TLR-4 and NF-κB expression. IPEC-J2 cells were untreated (Control), treated with 1 μg/mL LPS for 4 h (LPS), treated with 10 μg/mL CBF for 24 h (CBF), or treated with 10 μg/mL CBF for 20 h before exposure to 1 μg/mL LPS for 4 h (CBF + LPS). (A) Cytokine mRNA expression was analysed by qRT-PCR and is normalized to 18S ribosome protein mRNA. (B) Cytokines secretion of TNF-α, IL-8, IFN-γ in culture supernatants were measured by ELISA. (C) Protein levels of TLR-4, phosphorylated and total protein levels of p65 NF-κB, and GAPDH from cell lysates were determined by western blot analysis. Values represent the mean ± SEM of six independent assays. Within each gene, values without a common letter differ, *P* < 0.05.

two major TJ proteins that function in different epithelia [3], and the interaction between the COOH-terminal intracellular domain of occludin with ZO-1 is crucial for the organisation and stability of the TJ [47,49]. These proteins are directly involved in the regulation of paracellular barrier function [13,56]. Immunofluorescent staining of IPEC-J2 cell monolayers for occludin and ZO-1 demonstrated a distinct organisation of these proteins at the intercellular junctions, suggesting the presence of well-developed TJs in IPEC-J2 cell monolayers. LPS inhibited the localisation of occludin and ZO-1 to intercellular junctions and reduced

their mRNA and protein levels, suggesting that LPS increased permeability by disrupting TJs. CBF treatment prevented the LPS-induced downregulation of occludin and ZO-1 and caused the redistribution of these proteins to the cytoplasm and nucleus.

Disruption of the intestinal barrier induced by proinflammatory cytokines is associated with alterations in TJ protein expression [2]. The intestinal epithelial barrier function is frequently disrupted in acute or chronic enteropathies, such as inflammatory bowel disease, irritable bowel syndrome, and infectious diarrhea [34,43,54]. In the present

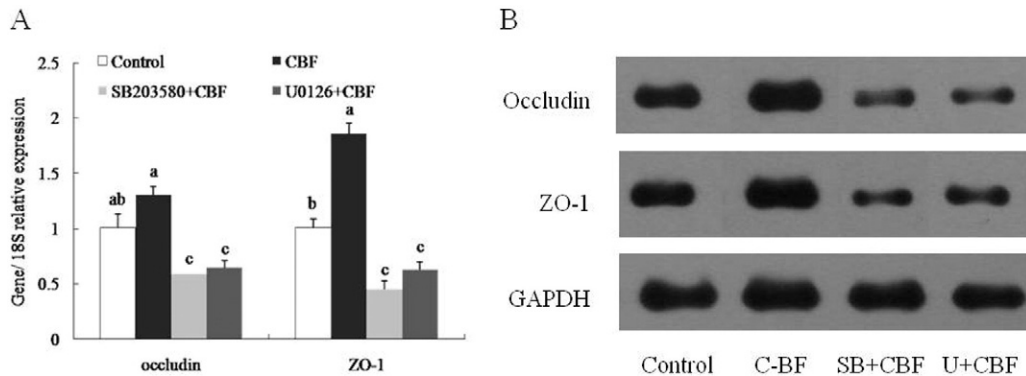


Fig. 7. MEK and p38 MAPK inhibitors block changes in the expression of adherens and tight junctions caused by CBF. qRT-PCR (A) and western blot (B) analysis of occludin and ZO-1 in IPEC-J2 cells treated with U0126 or SB203580 for 1 h before treatment with CBF for 24 h either alone or in combination. The signals were normalized to the expression of 18S ribosome protein mRNA. Values represent the mean ± SEM of six independent assays. Within each gene, values without a common letter differ, *P* < 0.05.

study, we showed that LPS rapidly disrupts barrier function in IPEC-J2 cell monolayers by downregulating and redistributing TJ proteins (ZO-1 and occludin) and increasing paracellular permeability to macromolecules. During the development of enteropathies, proinflammatory cytokines such as TNF- α , IL-8, and IFN- γ have been shown to disrupt intestinal epithelial barrier function both *in vitro* and *in vivo* [2,28]. Our study showed that LPS-induced intestinal barrier disruption was associated with the change of the morphology of TJs, the relocation of ZO-1 and occludin, and the release of proinflammatory cytokines (TNF- α , IL-8, and IFN- γ). TLR4 was upregulated in parallel with the upregulation of NF- κ B, IL-8, and TNF- α in IPEC-J2 in response to LPS, whereas its expression was unchanged in the CBF + LPS group. This result indicates that CBF inhibited the activation of TLR4 by LPS. There are two possible explanations for this finding. One possibility is that CBF binds to LPS and weakens the binding of LPS to TLR4. Another possible explanation is that CBF can directly shield the binding site of LPS. Stimulation with LPS for 4 h significantly upregulated the proinflammatory factors TNF- α , IFN- γ , and IL-8, and the mRNA levels of these cytokines were restored to normal levels by CBF pre-treatment for 20 h. In addition, CBF decreased the expression levels of NF- κ B (p65) induced by LPS. We speculate that CBF improves barrier function by indirectly regulating the abnormal expression of certain cytokines. These results were also proved by the previous results of our lab, which also demonstrated that C-BF significantly inhibited LPS-induced increases not only of serum TNF- α , but of TNF- α mRNA abundance in the small intestine. Meanwhile, LPS downregulated the expression of ZO-1 and occludin mRNA and protein, increasing intestinal permeability in mice [50]. Cytokines such as TNF- α , IFN- γ , and IL-8 are closely related to immune cell recruitment, which could lead to abnormal morphology of the intestine.

The MEK/p38 MAPK pathway is an intracellular signalling pathway that regulates a wide variety of physiological processes via serine/threonine phosphorylation cascades. p38 MAPK is ubiquitously expressed in all eukaryotic cells and regulates gene expression, mitosis, migration and apoptosis [6]. p38 MAPK activation is involved in the hydrogen peroxide-induced increase in endothelial and epithelial permeability [22]. Kevil et al. [21] indicated that MEK1 signalling increases paracellular permeability; however, some disparity exists in the observed cellular responses. Inhibition of MEK1 signalling had no effect on the expression of occludin or claudin-1 or affect TJ function in breast cancer cells [30]. Thus, the exact role of MAPKs in epithelial barrier function and TJs remains unclear, which could be due to cell specificity or the processing environment. In the present study, U0126 or SB203580 prevented the CBF-induced upregulation of ZO-1 and occludin, suggesting the involvement of the MEK and p38 MAPK pathways in TJ alterations caused by CBF. Several cathelicidin peptides bind to bacterial endotoxins and inactivate their biological activity [36,37]. This property has been used to reduce LPS mortality in murine models of endotoxaemia by application of LL-37/hCAP-18-derived peptides [25]. In contrast to the antimicrobial activity of the peptide, the uncleaved pro-peptide of rabbit CAP-18 blocks the biological activities of LPS [60]. Further investigation is necessary to determine whether the protective effect of CBF is mediated by its binding to LPS.

In conclusion, we report here for the first time that the antimicrobial peptide CBF has a protective effect on LPS-induced intestinal epithelial barrier disruption. The effects of CBF on barrier function mediated by the modulation of TJs in LPS-treated IPEC-J2 cell monolayers and the rat jejunum suggests its role as potential therapeutic agent for the prevention and management of LPS-related intestinal diseases in humans.

Funding

This work was supported by the Zhejiang Provincial Natural Science Foundation of China (under Grant number LY16C170001), National Natural Science Foundation of China (Grant number 31201809) and the earmarked fund for Modern Agro-industry Technology Research

System, China (Grant number CARS-36). The authors declare no competing financial interest.

Conflict of interest statement

The authors declare that there are no conflicts of interest.

Acknowledgments

We thank Dr. JJ Wang of China Agricultural University for supplying the IPEC-J2 cells used in the experiments.

References

- [1] D.M. Albin, J.E. Wubben, J.M. Rowlett, K.A. Tappenden, R.A. Nowak, Changes in small intestinal nutrient transport and barrier function after lipopolysaccharide exposure in two pig breeds, *J. Anim. Sci.* 85 (2007) 2517–2523.
- [2] M. Amasheh, I. Grotjohann, S. Amasheh, A. Fromm, J.D. Soderholm, M. Zeitz, et al., Regulation of mucosal structure and barrier function in rat colon exposed to tumor necrosis factor alpha and interferon gamma in vitro: a novel model for studying the pathomechanisms of inflammatory bowel disease cytokines, *Scand. J. Gastroenterol.* 44 (2009) 1226–1235.
- [3] J.M. Anderson, C.M. Van Itallie, Tight junctions and the molecular basis for regulation of paracellular permeability, *Am. J. Phys.* 269 (1995) G467–G475.
- [4] C. Arce, M. Ramirez-Boo, C. Lucena, J.J. Garrido, Innate immune activation of swine intestinal epithelial cell lines (IPEC-J2 and IPI-2I) in response to LPS from *Salmonella typhimurium*, *Comp. Immunol. Microbiol. Infect. Dis.* 33 (2010) 161–174.
- [5] R. Bals, J.M. Wilson, Cathelicidins—a family of multifunctional antimicrobial peptides, *Cell. Mol. Life Sci.* 60 (2003) 711–720.
- [6] M. Cargnello, P.P. Roux, Activation and function of the MAPKs and their substrates, the MAPK-activated protein kinases, *Microbiol. Mol. Biol. Rev.* 75 (2011) 50–83.
- [7] A.C. Chin, A.N. Flynn, J.P. Fedwick, A.G. Buret, The role of caspase-3 in lipopolysaccharide-mediated disruption of intestinal epithelial tight junctions, *Can. J. Physiol. Pharmacol.* 84 (2006) 1043–1050.
- [8] A.C. Chin, D.A. Teoh, K.G. Scott, J.B. Meddings, W.K. Macnaughton, A.G. Buret, Strain-dependent induction of enterocyte apoptosis by *Giardia lamblia* disrupts epithelial barrier function in a caspase-3-dependent manner, *Infect. Immun.* 70 (2002) 3673–3680.
- [9] M.J. Ciancio, L. Vitrutti, A. Dhar, E.B. Chang, Endotoxin-induced alterations in rat colonic water and electrolyte transport, *Gastroenterology* 103 (1992) 1437–1443.
- [10] E. Dickinson, R. Tuncer, E. Nadler, P. Boyle, S. Alber, S. Watkins, et al., NOX, a novel nitric oxide scavenger, reduces bacterial translocation in rats after endotoxin challenge, *Am. J. Phys.* 277 (1999) G1281–G1287.
- [11] L.A. Ding, J.S. Li, Y.S. Li, N.T. Zhu, F.N. Liu, L. Tan, Intestinal barrier damage caused by trauma and lipopolysaccharide, *World J. Gastroenterol.* 10 (2004) 2373–2378.
- [12] U.H. Durr, U.S. Sudheendra, A. Ramamoorthy, LL-37, the only human member of the cathelicidin family of antimicrobial peptides, *Biochim. Biophys. Acta* 1758 (2006) 1408–1425.
- [13] M. Furuse, M. Hata, K. Furuse, Y. Yoshida, A. Haratake, Y. Sugitani, et al., Claudin-based tight junctions are crucial for the mammalian epidermal barrier: a lesson from claudin-1-deficient mice, *J. Cell Biol.* 156 (2002) 1099–1111.
- [14] R.L. Gallo, K.J. Kim, M. Bernfield, C.A. Kozak, M. Zanetti, L. Merluzzi, et al., Identification of CRAMP, a cathelin-related antimicrobial peptide expressed in the embryonic and adult mouse, *J. Biol. Chem.* 272 (1997) 13088–13093.
- [15] M.M. Geens, T.A. Niewold, Optimizing culture conditions of a porcine epithelial cell line IPEC-J2 through a histological and physiological characterization, *Cytotechnology* 63 (2011) 415–423.
- [16] G. Hecht, Innate mechanisms of epithelial host defense: spotlight on intestine, *Am. J. Phys.* 277 (1999) C351–C358.
- [17] T.C. Hing, S. Ho, D.Q. Shih, R. Ichikawa, M. Cheng, J. Chen, et al., The antimicrobial peptide cathelicidin modulates *Clostridium difficile*-associated colitis and toxin A-mediated enteritis in mice, *Gut* 62 (2013) 1295–1305.
- [18] M. Iimura, R.L. Gallo, K. Hase, Y. Miyamoto, L. Eckmann, M.F. Kagnoff, Cathelicidin mediates innate intestinal defense against colonization with epithelial adherent bacterial pathogens, *J. Immunol.* 174 (2005) 4901–4907.
- [19] X. Jin, C.H. Yu, G.C. Lv, Y.M. Li, Increased intestinal permeability in pathogenesis and progress of nonalcoholic steatohepatitis in rats, *World J. Gastroenterol.* 13 (2007) 1732–1736.
- [20] K.P. Keenan, D.D. Sharpnack, H. Collins, S.B. Formal, A.D. O'Brien, Morphologic evaluation of the effects of Shiga toxin and E coli Shiga-like toxin on the rabbit intestine, *Am. J. Pathol.* 125 (1986) 69–80.
- [21] C.G. Kevil, T. Oshima, B. Alexander, L.L. Coe, J.S. Alexander, H(2)O(2)-mediated permeability: role of MAPK and occludin, *Am. J. Phys. Cell Physiol.* 279 (2000) C21–C30.
- [22] C.G. Kevil, T. Oshima, J.S. Alexander, The role of p38 MAP kinase in hydrogen peroxide mediated endothelial solute permeability, *Endothelium* 8 (2001) 107–116.
- [23] J.M. Kim, L. Eckmann, T.C. Savidge, D.C. Lowe, T. Witthoft, M.F. Kagnoff, Apoptosis of human intestinal epithelial cells after bacterial invasion, *J. Clin. Invest.* 102 (1998) 1815–1823.
- [24] H. Kimura, N. Sawada, H. Tobioka, H. Isomura, Y. Kokai, K. Hirata, et al., Bacterial lipopolysaccharide reduced intestinal barrier function and altered localization of 7H6 antigen in IEC-6 rat intestinal crypt cells, *J. Cell. Physiol.* 171 (1997) 284–290.

- [25] T. Kirikae, M. Hirata, H. Yamasu, F. Kirikae, H. Tamura, F. Kayama, et al., Protective effects of a human 18-kilodalton cationic antimicrobial protein (CAP18)-derived peptide against murine endotoxemia, *Infect. Immun.* 66 (1998) 1861–1868.
- [26] H.W. Koon, D.Q. Shih, J. Chen, K. Bakirtzi, T.C. Hing, I. Law, et al., Cathelicidin signaling via the Toll-like receptor protects against colitis in mice, *Gastroenterology* 141 (2011) 1852–1863 e1–3.
- [27] J.Y. Li, Y. Lu, S. Hu, D. Sun, Y.M. Yao, Preventive effect of glutamine on intestinal barrier dysfunction induced by severe trauma, *World J. Gastroenterol.* 8 (2002) 168–171.
- [28] Q. Li, Q. Zhang, M. Wang, S. Zhao, J. Ma, N. Luo, et al., Interferon-gamma and tumor necrosis factor- α disrupt epithelial barrier function by altering lipid composition in membrane microdomains of tight junction, *Cell Immunol.* 126 (2008) 67–80.
- [29] Y.F. Liu, C. Luan, X. Xia, S. An, Y.Z. Wang, Antibacterial activity, cytotoxicity and mechanisms of action of cathelicidin peptides against enteric pathogens in weaning piglets, *Int. J. Pept. Res. Ther.* 17 (2011) 175–184.
- [30] R. Macek, K. Swisshelm, M. Kubbies, Expression and function of tight junction associated molecules in human breast tumor cells is not affected by the Ras-MEK1 pathway, *Cell. Mol. Biol.* 49 (2003) 1–11 (Noisy-le-grand).
- [31] J. MacFie, Enteral versus parenteral nutrition: the significance of bacterial translocation and gut-barrier function, *Nutrition* 16 (2000) 606–611.
- [32] Y.R. Mahida, S. Makh, S. Hyde, T. Gray, S.P. Borriello, Effect of Clostridium difficile toxin A on human intestinal epithelial cells: induction of interleukin 8 production and apoptosis after cell detachment, *Gut* 38 (1996) 337–347.
- [33] J.C. Marshall, N.V. Christou, J.L. Meakins, Small-bowel bacterial overgrowth and systemic immunosuppression in experimental peritonitis, *Surgery* 104 (1988) 404–411.
- [34] C. Martinez, A. Gonzalez-Castro, M. Vicario, J. Santos, Cellular and molecular basis of intestinal barrier dysfunction in the irritable bowel syndrome, *Gut Liver* 6 (2012) 305–315.
- [35] S. Mishima, D. Xu, E.A. Deitch, Increase in endotoxin-induced mucosal permeability is related to increased nitric oxide synthase activity using the Ussing chamber, *Crit. Care Med.* 27 (1999) 880–886.
- [36] I. Nagaoka, S. Hirota, F. Niyonsaba, M. Hirata, Y. Adachi, H. Tamura, et al., Cathelicidin family of antibacterial peptides CAP18 and CAP11 inhibit the expression of TNF- α by blocking the binding of LPS to CD14(+) cells, *J. Immunol.* 167 (2001) 3329–3338.
- [37] I. Nagaoka, S. Hirota, F. Niyonsaba, M. Hirata, Y. Adachi, H. Tamura, et al., Augmentation of the lipopolysaccharide-neutralizing activities of human cathelicidin CAP18/LL-37-derived antimicrobial peptides by replacement with hydrophobic and cationic amino acid residues, *Clin. Diagn. Lab. Immunol.* 9 (2002) 972–982.
- [38] F. Niyonsaba, H. Ushio, N. Nakano, W. Ng, K. Sayama, K. Hashimoto, et al., Antimicrobial peptides human beta-defensins stimulate epidermal keratinocyte migration, proliferation and production of proinflammatory cytokines and chemokines, *J. Invest. Dermatol.* 127 (2007) 594–604.
- [39] S.T. O'Dwyer, H.R. Michie, T.R. Ziegler, A. Revhaug, R.J. Smith, D.W. Wilmore, A single dose of endotoxin increases intestinal permeability in healthy humans, *Arch. Surg.* 123 (1988) 1459–1464.
- [40] J.M. Otte, A.E. Zdebik, S. Brand, A.M. Chromik, S. Strauss, F. Schmitz, et al., Effects of the cathelicidin LL-37 on intestinal epithelial barrier integrity, *Regul. Pept.* 156 (2009) 104–117.
- [41] D.K. Podolsky, Review article: healing after inflammatory injury—coordination of a regulatory peptide network, *Aliment. Pharmacol. Ther.* 14 (Suppl. 1) (2000) 87–93.
- [42] S. Resta-Lenert, K.E. Barrett, Live probiotics protect intestinal epithelial cells from the effects of infection with enteroinvasive Escherichia coli (EIEC), *Gut* 52 (2003) 988–997.
- [43] S.Y. Salim, J.D. Soderholm, Importance of disrupted intestinal barrier in inflammatory bowel diseases, *Falk Symp.* 17 (2011) 362–381.
- [44] P. Schierack, M. Nordhoff, M. Pollmann, K.D. Weyrauch, S. Amasheh, U. Lodemann, et al., Characterization of a porcine intestinal epithelial cell line for in vitro studies of microbial pathogenesis in swine, *Histochem. Cell Biol.* 125 (2006) 293–305.
- [45] L.D. Schmidt, L.J. Kohrt, D.R. Brown, Comparison of growth phase on Salmonella enterica serovar Typhimurium invasion in an epithelial cell line (IPEC J2) and mucosal explants from porcine small intestine, *Comp. Immunol. Microbiol. Infect. Dis.* 31 (2008) 63–69.
- [46] R. Shaykhiyev, C. Beisswenger, K. Kandler, J. Senske, A. Puchner, T. Damm, et al., Human endogenous antibiotic LL-37 stimulates airway epithelial cell proliferation and wound closure, *Am. J. Phys. Lung Cell. Mol. Phys.* 289 (2005) L842–L848.
- [47] P. Sheth, S. Basuroy, C. Li, A.P. Naren, R.K. Rao, Role of phosphatidylinositol 3-kinase in oxidative stress-induced disruption of tight junctions, *J. Biol. Chem.* 278 (2003) 49239–49245.
- [48] P. Sheth, N. Delos Santos, A. Seth, N.F. LaRusso, R.K. Rao, Lipopolysaccharide disrupts tight junctions in cholangiocyte monolayers by a c-Src-, TLR4-, and LBP-dependent mechanism, *Am. J. Physiol. Gastrointest. Liver Physiol.* 293 (2007) G308–G318.
- [49] I. Simonovic, J. Rosenberg, A. Koutsouris, G. Hecht, Enteropathogenic Escherichia coli dephosphorylates and dissociates occludin from intestinal epithelial tight junctions, *Cell. Microbiol.* 2 (2000) 305–315.
- [50] D. Song, X. Zong, H. Zhang, T. Wang, H. Yi, C. Luan, et al., Antimicrobial peptide Cathelicidin-BF prevents intestinal barrier dysfunction in a mouse model of endotoxemia, *Int. Immunopharmacol.* 25 (2015) 141–147.
- [51] H.L. Song, S. Lv, P. Liu, The roles of tumor necrosis factor- α in colon tight junction protein expression and intestinal mucosa structure in a mouse model of acute liver failure, *BMC Gastroenterol.* 9 (2009) 70.
- [52] T. Sugiyama, T. Tashiro, H. Yamamori, K. Takagi, N. Hayashi, T. Itabashi, et al., Effects of total parenteral nutrition on endotoxin translocation and extent of the stress response in burned rats, *Nutrition* 15 (1999) 570–575.
- [53] X.Q. Sun, X.B. Fu, R. Zhang, Y. Lu, Q. Deng, X.G. Jiang, et al., Relationship between plasma D(-)-lactate and intestinal damage after severe injuries in rats, *World J. Gastroenterol.* 7 (2001) 555–558.
- [54] T. Suzuki, Regulation of intestinal epithelial permeability by tight junctions, *Cell. Mol. Life Sci.* 70 (2013) 631–659.
- [55] E.K. Tai, W.K. Wu, H.P. Wong, E.K. Lam, L. Yu, C.H. Cho, A new role for cathelicidin in ulcerative colitis in mice, *Exp. Biol. Med.* 232 (2007) 799–808 (Maywood).
- [56] S. Tsukita, M. Furuse, M. Itoh, Multifunctional strands in tight junctions, *Nat. Rev. Mol. Cell Biol.* 2 (2001) 285–293.
- [57] P. Valenti, R. Greco, G. Pitari, P. Rossi, M. Ajello, G. Melino, et al., Apoptosis of Caco-2 intestinal cells invaded by Listeria monocytogenes: protective effect of lactoferrin, *Exp. Cell Res.* 250 (1999) 197–202.
- [58] S.J. van Deventer, J.W. ten Cate, G.N. Tytgat, Intestinal endotoxemia. Clinical significance, *Gastroenterology* 94 (1988) 825–831.
- [59] Y. Wang, J. Hong, X. Liu, H. Yang, R. Liu, J. Wu, et al., Snake cathelicidin from *Bungarus fasciatus* is a potent peptide antibiotics, *PLoS One* 3 (2008), e3217.
- [60] K.A. Zarembek, S.S. Katz, B.F. Tack, L. Doukhan, J. Weiss, P. Elsbach, Host defense functions of proteolytically processed and parent (unprocessed) cathelicidins of rabbit granulocytes, *Infect. Immun.* 70 (2002) 569–576.
- [61] H. Zhang, X. Xia, F. Han, Q. Jiang, Y. Rong, D. Song, et al., Cathelicidin-BF, a novel antimicrobial peptide from *Bungarus fasciatus*, attenuates disease in a dextran sulfate sodium model of colitis, *Mol. Pharm.* 12 (2015) 1648–1661.